

Probing New Physics with Pulsar Timing Arrays

Zu-Cheng Chen (陈祖成)

Done with Yan-Chen Bi, Qing-Guo Huang, Jun Li, Lang Liu, Zhu Yi,
Chen Yuan, You Wu, Yu-Mei Wu

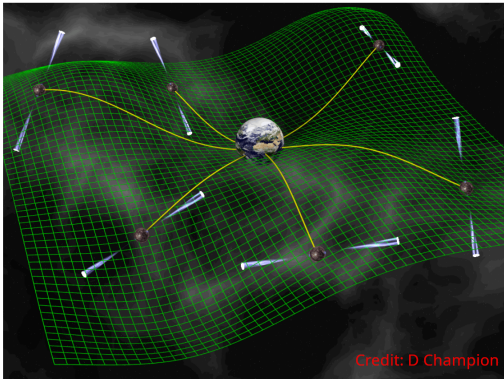
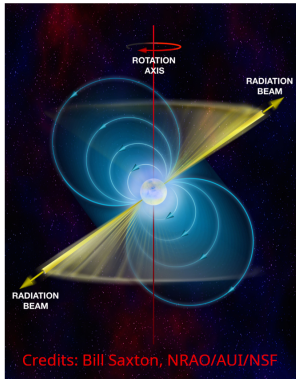
Based on PRL 124 (2020) 25, 251101; PRD 109 (2024) 6, L061301;
JCAP 11 (2023) 071; JCAP 04 (2024) 011; PRD 109 (2024) 6, L061101;
2401.09818 (PRDL); 2310.11238 (PRD)

2024-04-19 @ “引力的经典与量子性质”项目启动会



湖南师范大学
HUNAN NORMAL UNIVERSITY

Pulsar and pulsar timing array (PTA)



- Pulsars are highly magnetized, rotating neutron stars that emit regular pulses of electromagnetic radiation.
- GWs can cause tiny distortion in spacetime inducing variations in the time of arrivals (ToAs).
- A PTA pursues to detect nHz GWs by regularly monitoring ToAs from an array of the ultra rotational stable millisecond pulsars.

PTAs in operation



IPTA: PPTA + EPTA + NANOGrav + InPTA

Observers: CPTA, MPTA

Detecting a GWB with PTA

- Assume the GWB is isotropic, unpolarized, and stationary

$$\left\langle h_A^*(f, \hat{\Omega}) h_{A'}(f', \hat{\Omega}') \right\rangle = \frac{3H_0^2}{32\pi^3 f^3} \delta^2(\hat{\Omega}, \hat{\Omega}') \delta_{AA'} \delta(f - f') \Omega_{\text{gw}}(f)$$

- Spectrum of GWB

$$\Omega_{\text{gw}}(f) \equiv \frac{1}{\rho_{\text{crit}}} \frac{d\rho_{\text{gw}}}{d \ln f}, \quad \rho_{\text{crit}} = \frac{3H_0^2}{8\pi}, \quad \rho_{\text{gw}} = \frac{1}{32\pi} \left\langle \dot{h}_{ij}(t, \vec{x}) \dot{h}^{ij}(t, \vec{x}) \right\rangle,$$

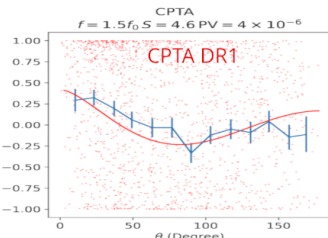
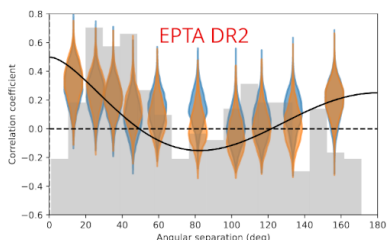
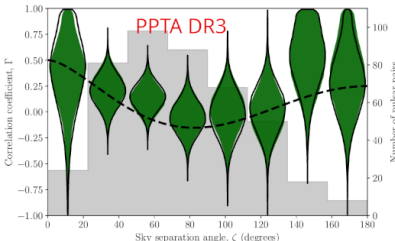
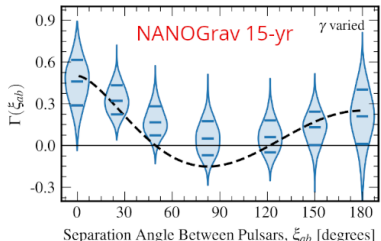
- Cross-power spectral density

$$S_{IJ} = \left\langle \tilde{r}_I^*(f) \tilde{r}_J(f') \right\rangle = \frac{1}{\gamma} \frac{H_0^2}{16\pi^4 f^5} \delta(f - f') \Gamma_{IJ}(f, L_I, L_J, \xi) \Omega_{\text{gw}}(f)$$

- Helling & Downs correlations for $fL \gg 1$ (short-wavelength approximation)

$$\Gamma_{IJ} = \frac{3}{2} \left(\frac{1 - \cos \xi}{2} \right) \ln \frac{1 - \cos \xi}{2} - \frac{1 - \cos \xi}{8} + \frac{1}{2}$$

The stochastic signal in PTAs (2023-06-29)



NANOGrav, 951 (2023) 1, L8; PPTA, ApJL 951 (2023) 1, L6

EPTA+InPTA, A&A 678 (2023) A50; CPTA, RAA 23 (2023) 7, 075024

SIGWs can explain the PTA signal.

9

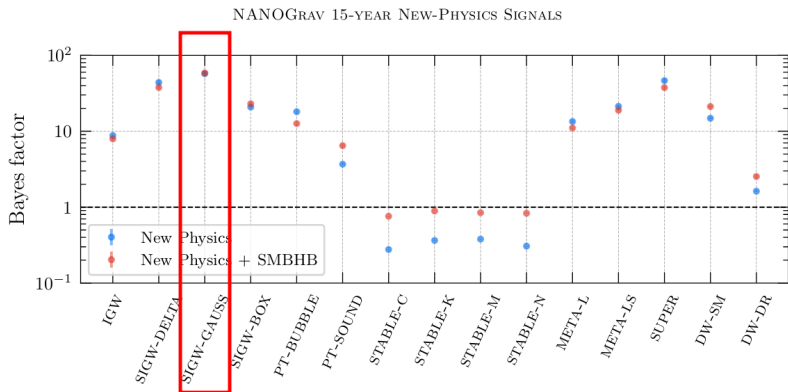


Figure 2. Bayes factors for the model comparisons between the new-physics interpretations of the signal considered in this work and the interpretation in terms of SMBHBs alone. Blue points are for the new physics alone, and red points are for the new physics in combination with the SMBHB signal. We also plot the error bars of all Bayes factors, which we obtain following the bootstrapping method outlined in Section 3.2. In most cases, however, these error bars are small and not visible.

Scalar-Induced Gravitational Waves (SIGWs)

- Primordial perturbations can be generated by quantum fluctuations during inflation.
- Metric perturbation in Newtonian gauge

$$ds^2 = a^2 \left\{ -(1 + 2\phi)d\eta^2 + \left[(1 - 2\phi)\delta_{ij} + \frac{h_{ij}}{2} \right] dx^i dx^j \right\}, \quad (1)$$

where $\phi \equiv \phi^{(1)}$ and $h_{ij} \equiv h_{ij}^{(2)}$ are the scalar and tensor perturbations, respectively.

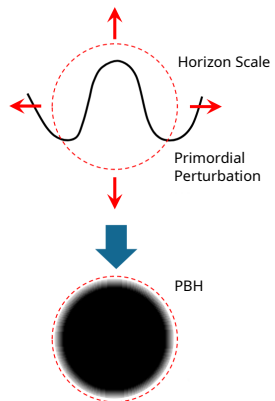
- Primordial scalar perturbation can be the source of SIGWs, as well as primordial black holes (PBHs).

Primordial black holes (PBHs)

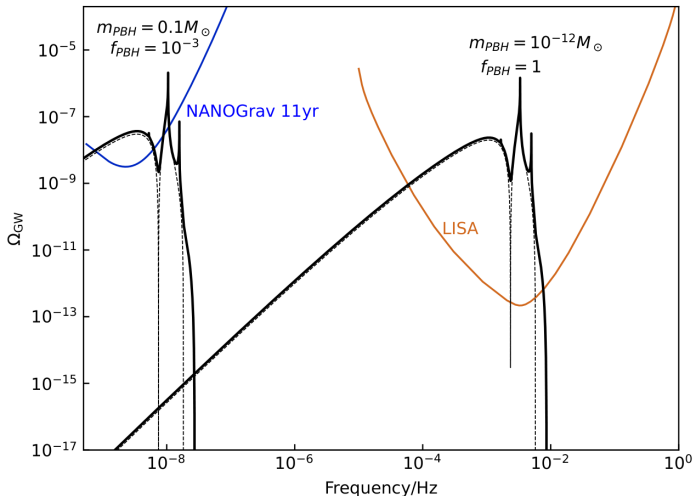
- PBHs are formed in the early universe by gravitational collapse of primordial density perturbations
- PBH mass can span many orders

$$m_{\text{PBH}} \sim \frac{t}{G} \sim 10^{-18} \left(\frac{t}{10^{-23}} \right) M_{\odot} \quad (2)$$

- PBHs survived from Hawking radiation can be DM candidates.
- PBHs can explain LVK BBHs.



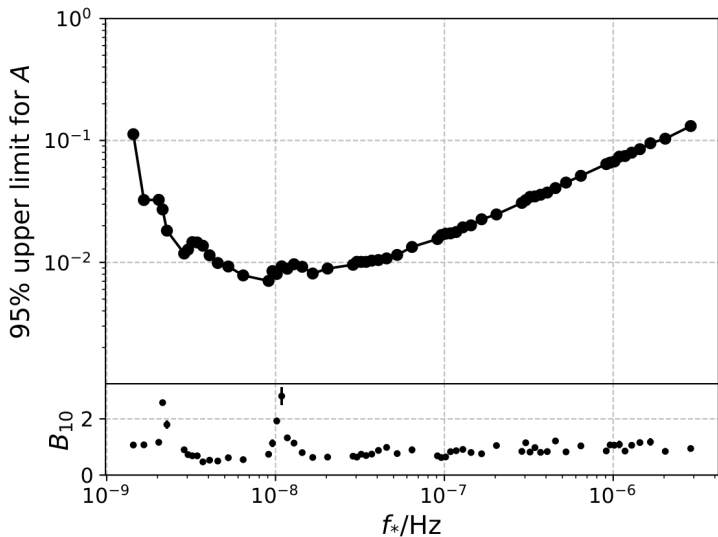
Detecting SIGW with PTA



Chen Yuan, ZCC, Qing-Guo Huang, PRD (Rapid Communications) 100 (2019) 8, 081301

See also: Rong-Gen Cai, Shi Pi, Shao-Jiang Wang, Xing-Yu Yang, JCAP 10 (2019) 059

Constrain SIGWs with NANOGrav 11-yr data set



ZCC, Chen Yuan, Qing-Guo Huang, PRL 124 (2020) 25, 251101

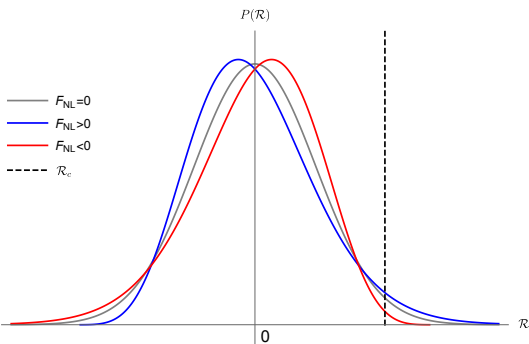
Non-Gaussianity

- The local-type non-Gaussian curvature perturbations:

$$\mathcal{R}(\vec{x}) = \mathcal{R}_G(\vec{x}) + F_{NL} (\mathcal{R}_G^2(\vec{x}) - \langle \mathcal{R}_G^2(\vec{x}) \rangle). \quad (3)$$

- The effective curvature power spectrum

$$P_{\mathcal{R}}^{\text{NG}} = P_{\mathcal{R}}(k) + F_{NL}^2 \int_0^\infty dv \int_{|1-v|}^{1+v} du \frac{P_{\mathcal{R}}(uk)P_{\mathcal{R}}(vk)}{2u^2v^2}. \quad (4)$$



Non-Gaussianity

- Power spectrum

$$P_{\mathcal{R}}(k) = \frac{A}{\sqrt{2\pi}\Delta} \exp\left(-\frac{\ln^2(k/k_*)}{2\Delta^2}\right). \quad (5)$$

- The energy density of GWs

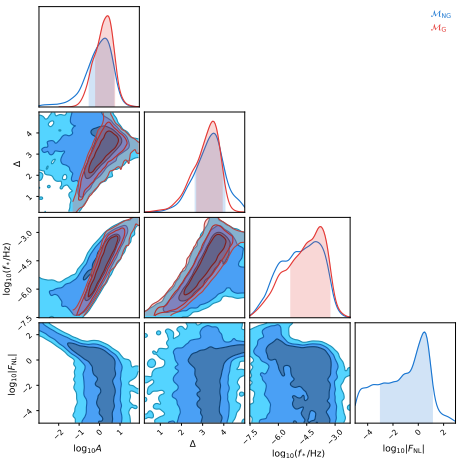
$$\Omega_{\text{GW}}(k) = \int_0^\infty dv \int_{|1-v|}^{|1+v|} du \mathcal{T} P_{\mathcal{R}}^{\text{NG}}(vk) P_{\mathcal{R}}^{\text{NG}}(uk), \quad (6)$$

where the transfer function $\mathcal{T} = \mathcal{T}(u, v)$ is given by

$$\begin{aligned} \mathcal{T}(u, v) = & \frac{3}{1024v^8u^8} \left[4v^2 - (v^2 - u^2 + 1)^2 \right]^2 (v^2 + u^2 - 3)^2 \\ & \times \left\{ \left[(v^2 + u^2 - 3) \ln \left(\left| \frac{3 - (v+u)^2}{3 - (v-u)^2} \right| \right) - 4vu \right]^2 \right. \\ & \left. + \pi^2 (v^2 + u^2 - 3)^2 \Theta(v + u - \sqrt{3}) \right\}. \end{aligned} \quad (7)$$

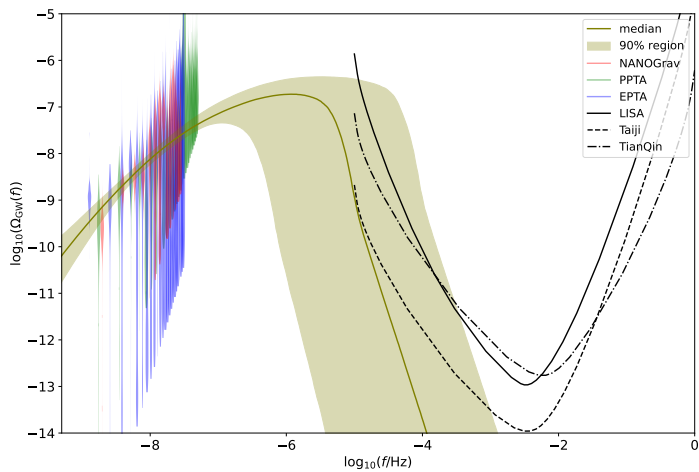
Rong-gen Cai, Shi Pi, Misao Sasaki, PRL 122 (2019) 20, 201101

PE with NANOGrav 15-yr data set + PPTA DR3 + EPTA DR2



- $|F_{\text{NL}}| \lesssim 13.9$
- $-13.9 \lesssim F_{\text{NL}} \lesssim -0.1$ when further requiring $f_{\text{PBH}} \lesssim 1$.

Lang Liu, ZCC, Qing-Guo Huang, PRD 109 (2024) 6, L061301



Implications

- The constraints on F_{NL} have significant implications for multi-field inflation models.
- For instance, adiabatic curvaton models predict that

$$f_{\text{NL}} = \frac{5}{3} F_{\text{NL}} = \frac{5}{4r_D} - \frac{5r_D}{6} - \frac{5}{3}, \quad (8)$$

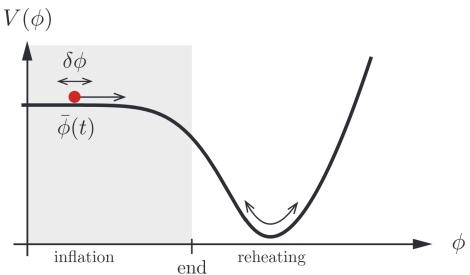
where $r_D = 3\rho_{\text{curvaton}}/(3\rho_{\text{curvaton}} + 4\rho_{\text{radiation}})$ represents the “curvaton decay fraction” at the time of curvaton decay.

- Our constraint $-13.9 \lesssim F_{\text{NL}} \lesssim -0.1$ implies

$$r_D \gtrsim 0.62 \quad (95\%), \quad (9)$$

indicating that the curvaton field has a non-negligible energy density when it decays.

Equation of state of the early Universe

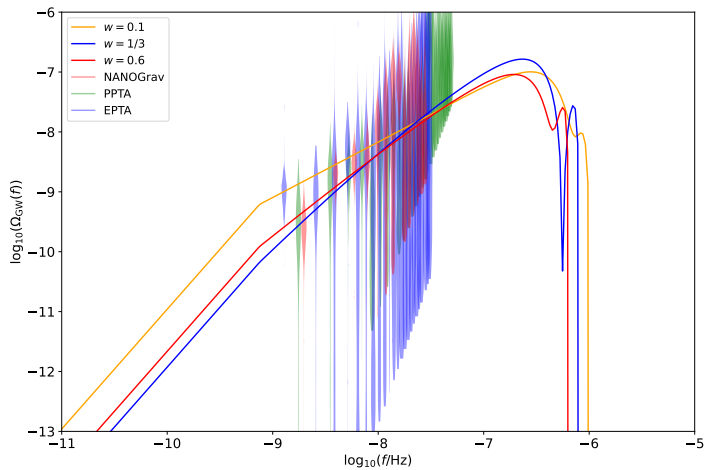


- The SIGW spectrum for the scales $k \gtrsim k_{\text{rh}}$ is

$$\Omega_{\text{GW},\text{rh}} = \left(\frac{k}{k_{\text{rh}}}\right)^{-2b} \int_0^\infty dv \int_{|1-v|}^{1+v} du \mathcal{T}(u, v, w) \mathcal{P}_{\mathcal{R}}(ku) \mathcal{P}_{\mathcal{R}}(kv), \quad (10)$$

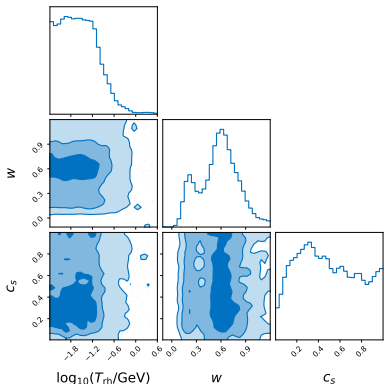
where $b \equiv (1 - 3w)/(1 + 3w)$. And $\Omega_{\text{GW},\text{rh}} \propto (k/k_{\text{rh}})^2$ when $k \lesssim k_{\text{rh}}$.

Guillem Domènech, Shi Pi, Misao Sasaki, JCAP 08 (2020) 017



Lang Liu, ZCC, Qing-Guo Huang, 2307.14911

PE with NANOGrav 15-yr data set + PPTA DR3 + EPTA DR2



- Reheating temperature $T_{\text{rh}} \lesssim 0.2 \text{ GeV}$.
- $w < 0$ is excluded at 95% CL.
- $w = 1/3$ is consistent with the PTA data.
- w peaks at around 0.6.
- Since during the oscillation of inflaton, $w = \frac{p-2}{p+2}$ for a potential $V(\phi) \propto \phi^p$, then, it implies a $V(\phi) \propto \phi^8$.

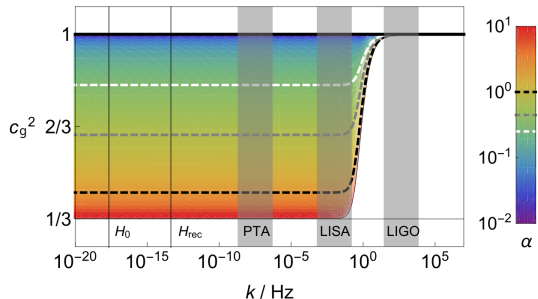
Lang Liu, ZCC, Qing-Guo Huang, JCAP 11 (2023) 071

Speed of GW

- GW170817: $-3 \times 10^{-15} \leq c_g - 1 \leq 7 \times 10^{-16}$

[PRL 119 \(2017\) 16, 161101](#)

- c_g can be frequency dependent



[Claudia de Rham, Scott Melville, PRL 121 \(2018\) 22, 221101](#)

Speed of SIGW

- EoM

$$h_{\mathbf{k}}''(\eta) + 2\mathcal{H}h_{\mathbf{k}}'(\eta) + \textcolor{red}{c_g^2}k^2h_{\mathbf{k}}(\eta) = 4S_{\mathbf{k}}(\eta). \quad (11)$$

- SIGW spectrum

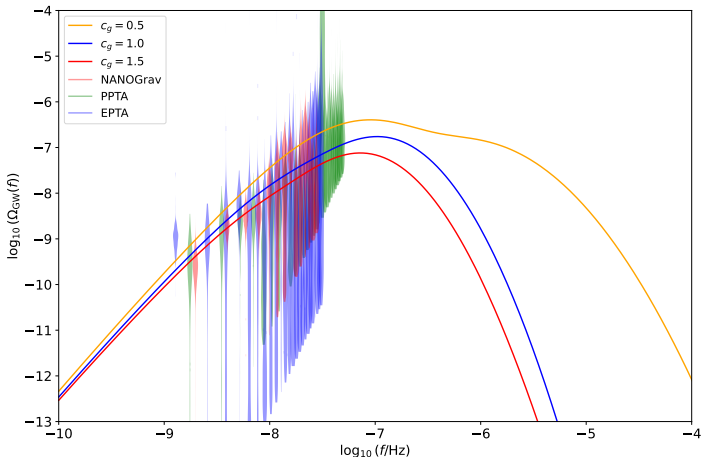
$$\Omega_{\text{GW}}(k) = \int_0^\infty dv \int_{|1-v|}^{1+v} du \mathcal{T}(u, v, \textcolor{red}{c_g}) P_\zeta(vk) P_\zeta(uk). \quad (12)$$

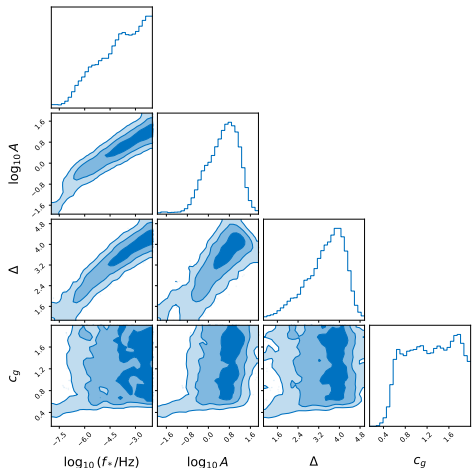
- Transfer function

$$\begin{aligned} \mathcal{T}(u, v, c_g) &= \frac{3 \left[4v^2 - (v^2 - u^2 + 1)^2 \right]^2 (v^2 + u^2 - 3c_g^2)^2}{1024v^8u^8} \\ &\times \left\{ \left[(v^2 + u^2 - 3c_g^2) \ln \left(\left| \frac{3c_g^2 - (v+u)^2}{3c_g^2 - (v-u)^2} \right| \right) - 4vu \right]^2 \right. \\ &\quad \left. + \pi^2 (v^2 + u^2 - 3c_g^2)^2 \Theta(v+u-\sqrt{3}c_g) \right\}. \end{aligned} \quad (13)$$

Jun Li, Guang-Hai Guo, 2312.04589

PE with NANOGrav 15-yr data set + PPTA DR3 + EPTA DR2

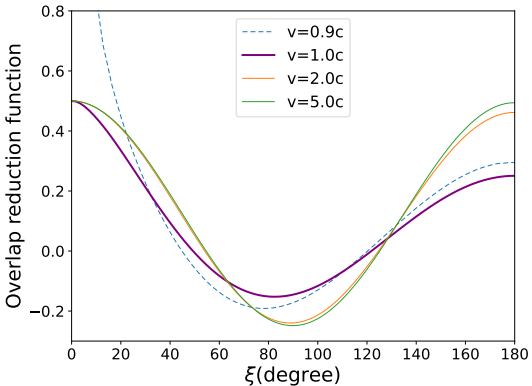




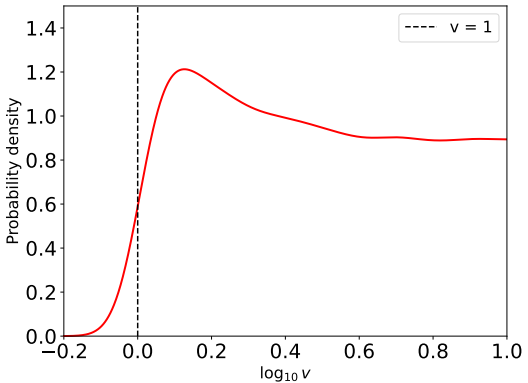
- $c_g \gtrsim 0.61$ at a 95% CI.
- Consistent with $c_g = 1$.

ZCC, Jun Li, Lang Liu, Zhu Yi, 2401.09818 (PRDL accepted)

ORF



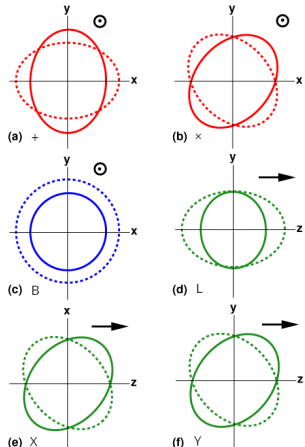
PE with NANOGrav 15-yr data set



- $c_g \gtrsim 0.85$.
- Still consistent with $c_g = 1$.

Alternative Polarizations

Gravitational-Wave Polarization



- A general metric gravity theory in 4D spacetime can have 6 polarization modes.
- polarization tensors

$$\epsilon_{ij}^+ = \hat{m} \otimes \hat{m} - \hat{n} \otimes \hat{n},$$

$$\epsilon_{ij}^x = \hat{m} \otimes \hat{n} + \hat{n} \otimes \hat{m},$$

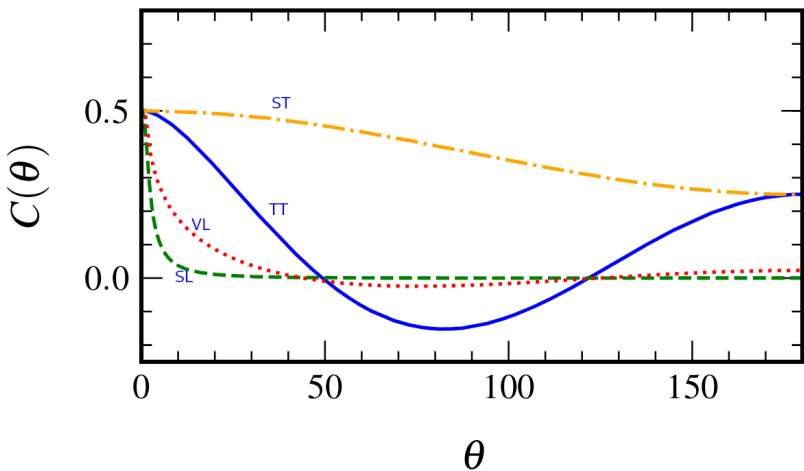
$$\epsilon_{ij}^B = \hat{m} \otimes \hat{m} + \hat{n} \otimes \hat{n},$$

$$\epsilon_{ij}^L = \hat{\Omega} \otimes \hat{\Omega},$$

$$\epsilon_{ij}^X = \hat{m} \otimes \hat{\Omega} + \hat{\Omega} \otimes \hat{m},$$

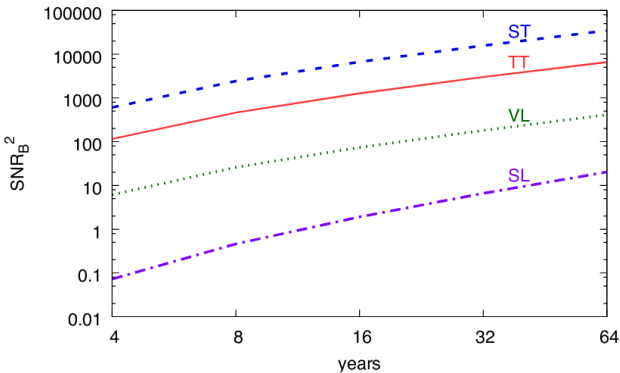
$$\epsilon_{ij}^Y = \hat{n} \otimes \hat{\Omega} + \hat{\Omega} \otimes \hat{n}$$

ORF



$$|\Gamma_{ST}| > |\Gamma_{TT}| > |\Gamma_{VL}| > |\Gamma_{SL}|$$

$$\text{SNR}_B^2 = 2 \sum_f \sum_a^{N_p} \sum_{b>a}^{N_p} \frac{\Gamma_{ab}^I(f)}{\Gamma_{aa}^I(f)\Gamma_{bb}^I(f) + \Gamma_{ab}^I(f)}.$$



ST is the easiest to detect among the four polarization modes.

Neil J. Cornish, Logan O'Beirne, Stephen R. Taylor, Nicolás Yunes, PRL 120 (2018)

Search for alternative polarizations in NANOGrav 15-yr data set

- Our paper appeared on arXiv one day prior to NANOGrav's. Both sets of results are broadly consistent with each other.
- [ZCC, Yu-Mei Wu, Yan-Chen Bi, Qing-Guo Huang, 2310.11238 \(PRD accepted\)](#)

Model	ST	VL	SL	GTb	TT + ST
BF	0.40(3)	0.12(2)	0.002(1)	3.9(3)	0.943(5)

- [NANOGrav Collaboration, ApJ 964 \(2024\) 1, L14](#)

Our Bayesian analyses show the Bayes factor for HD over ST is ~ 2 , and the Bayes factor for a model with both correlations compared to a model with just HD is ~ 1 . These results are largely consistent with a similar study by Chen et al. (2023), in which they searched NANOGrav's 15 yr data set for nontensorial GWBs on a similar timescale to the work presented here. Taking the spectral parameter recovery into account, as in Figure 3, we found each correlation, when fit for individually, is in agreement with CURN. We also found more informative $\log_{10} A_g$ and γ_g recovery for HD than ST, and HD parameters show better agreement with CURN spectral parameters when correlations are included together. The analyses in this Letter, as well as those in Bernardo & Ng (2023c) and Chen et al. (2023), do not rule out the possibility of ST correlations in our data. However, our analysis also shows no statistical need for an additional stochastic process with ST correlations.

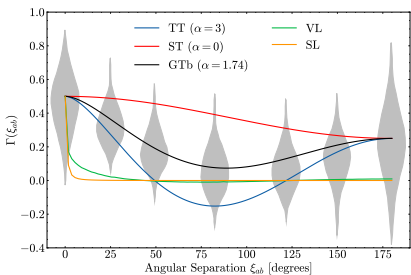
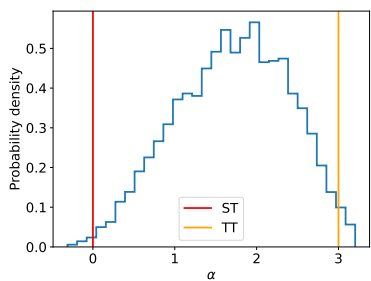
We also consider a parameterized transverse ORF as

$$\Gamma_{ab}(f) = \frac{1}{8} (3 + 4\delta_{ab} + \cos \xi_{ab}) + \frac{\alpha}{2} k_{ab} \ln k_{ab}. \quad (14)$$

ST: $\alpha = 0$

TT: $\alpha = 3$

prior of α : Uniform(-10, 10)



- Our analysis yields $\alpha = 1.74^{+1.18}_{-1.41}$, thus excluding both the TT and ST models at the 90% CL.

Summary

PTAs are promising tools for probing new physics, including:

- SIGW

ZCC, Chen Yuan, Qing-Guo Huang, PRL 124 (2020) 25, 251101

- Non-Gaussianity of curvature perturbations

Lang Liu, ZCC, Qing-Guo Huang, PRD 109 (2024) 6, L061301

- Equation of state of the early Universe

Lang Liu, ZCC, Qing-Guo Huang, JCAP 11 (2023) 071

Lang Liu, You Wu, ZCC, JCAP 04 (2024) 011

- Speed of GW

Yan-Chen Bi, Yu-Mei Wu, ZCC, Qing-Guo Huang, PRD 109 (2024) 6, L061101

ZCC, Jun Li, Lang Liu, Zhu Yi, 2401.09818 (PRDL accepted)

- Alternative polarizations

ZCC, Chen Yuan, Qing-Guo Huang, SCPMA 64 (2021) 12, 120412

Yu-Mei Wu, ZCC, Qing-Guo Huang, ApJ 925 (2022) 1, 37

ZCC, Yu-Mei Wu, Qing-Guo Huang, CTP 74 (2022) 10, 105402

ZCC, Yu-Mei Wu, Yan-Chen Bi, Qing-Guo Huang, 2310.11238 (PRD accepted)

- Graviton mass

Yu-Mei Wu, ZCC, Qing-Guo Huang, PRD 107 (2023) 4, 042003

Yu-Mei Wu, ZCC, Yan-Chen Bi, Qing-Guo Huang, CQG 41 (2024) 7, 075002

- ...